Distribution Agreement

In presenting this thesis as a partial fulfillment of the requirements for a degree from Emory University, I hereby grant to Emory University and its agents the non-exclusive license to archive, make accessible, and display my thesis in whole or in part in all forms of media, now or hereafter now, including display on the World Wide Web. I understand that I may select some access restrictions as part of the online submission of this thesis. I retain all ownership rights to the copyright of the thesis. I also retain the right to use in future works (such as articles or books) all or part of this thesis.

Mi Hyun Choi December 8, 2017

Anatomical survey of paravertebral sympathetic chain in adult mice

By

Mi Hyun (Hannah) Choi

Dr. Shawn Hochman

Adviser

Department of Neuroscience and Behavioral Biology

Dr. Shawn Hochman

Adviser

Dr. Michael Crutcher

Committee Member

Dr. Sandra Garraway

Committee Member

Dr. Leah Roesch

Committee Member

2017

Anatomical survey of paravertebral sympathetic chain in adult mice

By

Mi Hyun (Hannah) Choi

Dr. Shawn Hochman

Adviser

An abstract of
a thesis submitted to the Faculty of Emory College of Arts and Sciences
of Emory University in partial fulfillment
of the requirements of the degree of
Bachelor of Sciences with Honors

Department of Neuroscience and Behavioral Biology

2017

Abstract

Anatomical survey of paravertebral sympathetic chain in adult mice

By Mi Hyun Choi

The predominant purpose of thoracic paravertebral sympathetic ganglia (tPSG) is innervation of vasculature for control of vasomotor function. Despite this important function, anatomical and physiological properties of sympathetic postganglionic neuron (SPN) populations in the tPSG are not well-understood. Consequently, their role in vascular changes observed after injury or disease is barely known. Here, the numbers and diameters of two major SPN chemical phenotypes – cholinergic and noradrenergic – were determined along the rostrocaudal tPSG axis comprising segments T1-T13. I used immunohistochemistry to amplify GFP detection in choline acetyltransferase (ChAT) GFP-expressing cholinergic neurons and to detect tyrosine hydroxylase (TH) noradrenergic neurons. Mice averaged 13,107.5 neurons (n=2) but inter-animal variability in number was enormous (6,494 vs.19,721). Of these, 97.2% were noradrenergic and 2.8% were cholinergic. Examination of additional counts from 6 mice in select ganglia (T3, T5 and T9) supported a remarkable inter-animal variability in numbers counted that were not overtly sex related. The number of noradrenergic SPNs peaked at T7 and T8. The number of cholinergic SPNs was greater in rostral (T1-T6) compared to caudal segments (T7-T13; $p<0.001$), presumably due to preferential innervation for forepaw footpad sweat glands. Noradrenergic SPN diameter (17.5μm) was slightly but significantly larger than the average cholinergic SPN diameter (16.7μm; $p<0.0001$). Both noradrenergic mean cell diameter and cholinergic mean cell diameter differed significantly between segments ($p<0.0001$ for each). Overall, this study compared the numbers, diameters and segmental distribution of noradrenergic and cholinergic neurons in the sympathetic paravertebral thoracic chain of mice. Most notable observations were the expected dominance of adrenergic neurons and the remarkable variability on neurons numbers between animals.

Anatomical survey of paravertebral sympathetic chain in adult mice

By

Mi Hyun (Hannah) Choi

Dr. Shawn Hochman

Adviser

An abstract of
a thesis submitted to the Faculty of Emory College of Arts and Sciences
of Emory University in partial fulfillment
of the requirements of the degree of
Bachelor of Sciences with Honors

Department of Neuroscience and Behavioral Biology

2017

Table of Contents

List of Tables and Figures

INTRODUCTION

The efferent pathway of the sympathetic division of the autonomic nervous system involves a network of at least two neurons: preganglionic (**PreSNs**) and postganglionic neurons (**SPNs**) (Langley, 1921). The PreSNs, located in the thoracic and rostral lumbar spinal cord, integrate information from the central nervous system and project their axons via the ventral roots. They synapse onto the SPNs and transmit information through cholinergic neurotransmission, using the neurotransmitter acetylcholine (Dale, 1937). The SPNs subsequently relay the received signal to a variety of target tissues. A large population of SPNs is located in the paravertebral ganglia (**PSG**), with the remainder in the prevertebral ganglia (Figure 1A) (Burnstock, 1969). Most of the SPNs in the PSG are noradrenergic (Falck et al., 1962). That is, they release the neurotransmitter noradrenaline. Yet, about 4% of SPNs in the PSG are cholinergic, though the percentages differ among different species and different individuals (Weihe and Eiden, 2000; Koelle and Friedenwald, 1949; Masliukov and Timmermans, 2004) (Figure 1B). Subpopulations of noradrenergic and cholinergic SPNs also differ in their expression of neuropeptides (Ernsberger and Rohrer, 1999). The specific neurochemical phenotype of each subpopulation of SPNs is correlated with the functions they serve and their choice of innervating target (Gibbins, 1991; Gibbins 1992). The chemical coding of noradrenergic and cholinergic SPNs will be described in detail in the subsections on noradrenergic and cholinergic neurons.

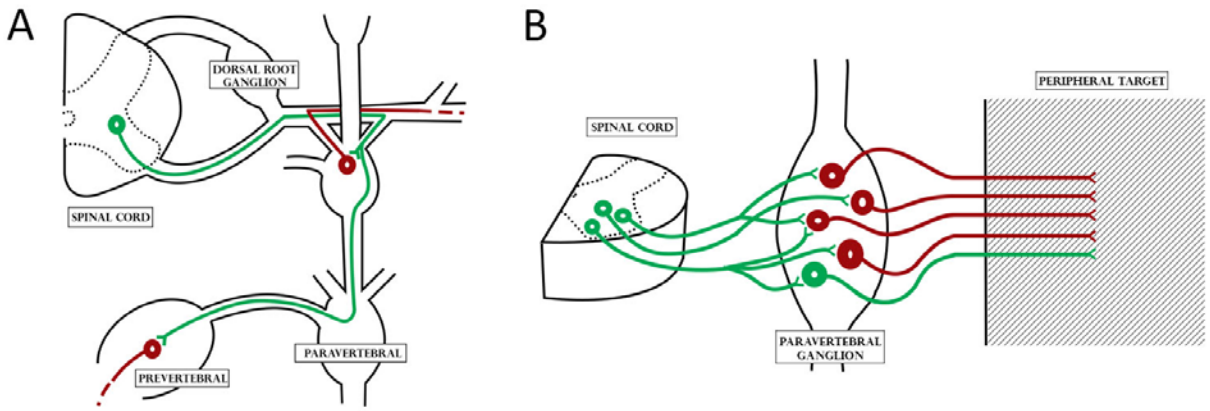

Figure 1. Schematic of autonomic sympathetic efferent pathway. Noradrenergic SPNs and fibers are shown in red, and cholinergic PreSN and SPN and fibers in green. A) The sympathetic efferent signal from PreSNs exits the spinal cord through the ventral root and reaches the SPNs in the sympathetic ganglia, either paravertebral or prevertebral (Burnstock, 1969). A paravertebral SPN is shown on the right and a prevertebral SPN is shown on the bottom left in red. The SPNs, in turn, transmit information to their peripheral target tissue. The red dashed lines indicate that the axons project farther towards the periphery. B) This is a more focused depiction of the sympathetic efferent pathway through the paravertebral ganglion. Cholinergic PreSNs innervate not only noradrenergic, but also cholinergic SPNs in the paravertebral ganglia (Falck et al., 1962). The PreSNs innervate several SPNs, and each SPN receives synaptic inputs from more than one PreSN. Each SPN innervates a specific target to perform its distinct regulatory role.

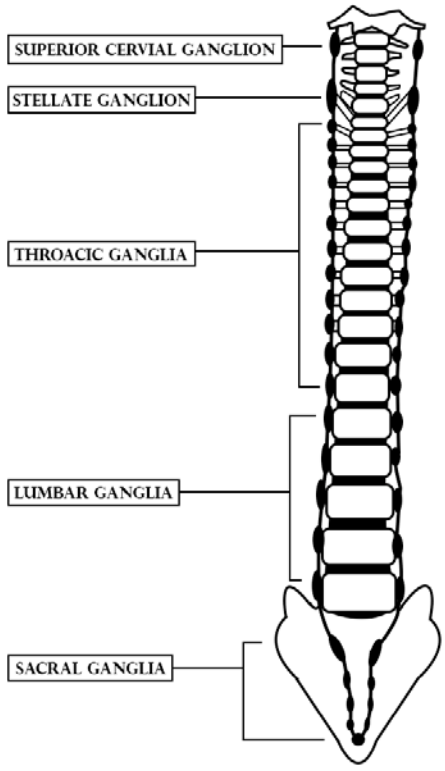

Figure 2. This figure shows the location of the sympathetic chains, shown in black, relative to the vertebrae. The chains are on either side of the vertebrae, consisting of paravertebral ganglia interconnected with interganglionic nerve segments (Elfvin et al., 1993). They stretch from the rostral cervical region to the caudal sacral region. Each ganglion lies ventral to a rib, and is enmeshed in adherent fat. The level of each ganglion corresponds to the level of the spinal column they are adjacent to. The SPNs are organized into segmental units. Each ganglion is referred to as their segmental level (e.g. a T5 ganglion), with the exception of superior cervical ganglion, the stellate ganglion, and ganglion impar (not labeled: the most caudal ganglion joining the two chains). The number of ganglia within each region distinguished by the labels in the figure vary among different species and also among individuals within the same species. In mice, generally, the superior cervical ganglion is present in the upper cervical area. The stellate ganglion is a fusion of the most caudal cervical and most rostral thoracic ganglia (T1). There are thirteen thoracic ganglia, 6 lumbar ganglia, 4 sacral ganglia and the ganglion impar. In humans, there are superior cervical ganglion, middle cervical ganglion, inferior cervical ganglion, 12 thoracic ganglia, 5 lumbar ganglia, 5 sacral ganglia and ganglion impar. The SPNs in each ganglion are innervated by PreSN fibers originating from different segments of the spinal cord, not necessarily located at the same segmental level. The PreSN fibers either directly innervate the ganglion on the same level or ascend and/or descend via the interganglionic nerve about 3 ganglia before innervating on a SPN (Blackman and Purves, 1969). Each subpopulation of SPNs in each ganglion has its own specialized function and innervates a unique peripheral target (Naftel and Hardy, 1997).

Size is another factor that varies considerably among SPNs of different functions (Gibbins, 1991). A number of basic physiological processes – such as metabolic flux, biosynthetic capacity, and nutrient exchange – occur on the cell surface, and are thus related to cell size (Marshall et al., 2012). Therefore, cell size is an important parameter to be studied in cells. The cell body size of SPNs is especially important, because it is crucial to understanding the inputs to and the outputs from these cells (Gibbins, 1991). In mammals, though there is a significant variation in cell size among different species, the cell body size of SPNs within each species is correlated with functional characteristics, such as dendritic arborization complexity, number of synaptic inputs and volume of target tissue (Purves and Lichtman, 1985; Gibbins et al., 1991; Boyd et al., 1996; Gibbins et al., 1998; Purves and Hume, 1981; Voyvodic, 1987). A study in bullfrog showed that it was possible to identify SPNs of different function with 94-96% accuracy just by measuring their sizes (Dodd and Horn, 1983). The size of SPNs may serve an additional marker of SPN phenotypes in the PSG.

The PSG are connected via interganglionic nerve segments, forming two sympathetic chains that lie along either side of the vertebrae as shown in Figure 2 (Elfvin et al., 1993). Each chain is organized into cervical, thoracic, lumbar, sacral, and coccygeal regions corresponding to the levels of the spinal column they are adjacent to, although the number of ganglia within each segment varies among different species. Previous studies on the sympathetic chain have focused on exploring the more accessible cervical and lumbar ganglia (Gibbins, 1991; Klimaschewski et al., 1996, Li et al., 2007; Voyvodic, 1987; Wright, 1988; Asamoto, 2004; Beaston-Wimmer and Smolen, 1991; Gibbins et al., 1998). The thoracic paravertebral sympathetic ganglia (**tPSG**) have not been as thoroughly explored, in part, due to their inaccessibility. They are transparent

structures enmeshed in opaque adherent fat across the heads of corresponding ribs (Garry and Henry, 1949). The few studies on the tPSG focused only on specific segmental levels of the ganglia (Stellate and T5 – Lichtman et al., 1980; stellate – Masliukov and Timmermans, 2004, Holmstedt and Sjoqvist, 1959, Schafer et al., 1980; T5-T9 – Blackman and Purves, 1969), especially the stellate ganglia, or analyzed the data on the thoracic chain as a whole without making a distinction between the different thoracic levels (Schafer et al., 1998). A deeper understanding of the tPSG is crucial, as sympathetic control of vasomotor tone is predominantly controlled by the sympathetic signal through the SPNs that reside in the tPSG (Dehal et al., 1992; Elfvin et al., 1993). Autonomic dysreflexia observed after injury or onset of a disease is a potentially fatal condition characterized by episodes of hypertension in response to a strong noxious stimulus (Karlsson, 1999). While it is well known in animal models that afferent plasticity within the spinal cord relates to autonomic dysreflexia, it is not clear whether the plasticity within the tPSG contributes to the hypertensive reflex despite the fact that SPNs in the tPSG directly innervate the vasculature (Rabchevsky, 2006; Hou et al., 2009). Our lab is interested in studying the plasticity of SPNs in the tPSG after spinal cord injury. We hypothesize that the tPSG are more than simple relays and other mechanisms may exist (Janig et al, 1982). Identifying SPN populations according to different functional parameters and their distribution in the thoracic chain could be an invaluable precedent to future studies on this topic. A record of the cellular properties of the SPNs in the sympathetic chain can contribute to the advancement in the studies of the tPSG with respect to injury/disease-induced plasticity and autonomic dysreflexia.

Most of the work done focused on co-localizing various neuropeptides and the two classic neurotransmitters norepinephrine and acetylcholine in the SPNs, in the absence of knowledge of the exact distribution of the noradrenergic and cholinergic SPNs and the

distribution of different-sized SPNs, and thus the distribution of SPNs of different functions, along the chain (Elfvin et al., 1993). In addition to differences in neurotransmitter content and size, the location of the SPNs along the rostrocaudal axis has been shown to be relevant to the different functional pathway of SPNs (Forehand, 1994). It is important to distinguish SPNs of different segmental origins from one another, since they each receive a unique PreSN signals and innervate a unique target according to its location along the rostrocaudal axis (Lichtman et al., 1980). The innervations on SPNs display a complicated convergence and divergence patterns, with PreSNs innervating multiple SPNs and SPNs receiving presynaptic input from multiple PreSNs. Electrophysiological studies in mammals have shown that more rostral PSG are innervated by more rostral thoracic PreSNs, and more caudal PSG by more caudal thoracic PreSNs (Nja and Purves, 1977; Lichtman et al., 1979; Yip, 1986). PreSNs identify SPNs by some topographic identity (Nja and Purves, 1978; Purves et al., 1981). Thus, depending on the location of the SPNs, they are innervated by PreSNs of different origins and thus different function. A detailed knowledge of the distribution of the synaptic inputs the SPNs receive could help us confirm that the SPNs have modulatory functions that characterize them as more than relay stations (Gibbins et al., 2000). The SPN outputs also show convergence at the target organs (McLachlan, 2003). Denervation, axonal tracing, and immunohistochemistry studies showed that the PSG are subdivided into regions of SPNs that project to specific targets throughout the body (Jacobwitz and Woodward, 1968; Matthews and Raisman, 1972; Bowers and Zigmond, 1979; Flett and Bell, 1991; Lindh et al., 1986a). Although some neurons dispersed along the rostrocaudal axis may release the same neurotransmitters, they may act on different targets, thus being parts of different subpopulations depending on which ganglion they reside in. For example, noradrenergic vasocontrictor SPNs in a thoracic ganglion were shown to express a

characteristic suite of ion channels different from that expressed by noradrenergic vasoconstrictor SPNs in the superior cervical ganglion (Jobling and Gibbins, 1999). The distribution within each ganglion could also be an indication of the innervation target, as revealed by retrograde tracing that showed that the SPNs innervating a specific target are clustered together on a specific side of the ganglion (Nozdrachev, 2002; Hill and Elde, 1989). The distinct roles of subpopulations of SPNs on their targets are thus influenced by their location along the rostrocaudal axis (Elfvin, 1993).

There have been precedents to this study that distinguished functions of SPNs based on the functional markers of our interest: neurochemical phenotype and size (Gibbins, 1991; Gibbins, 1992). Studies on the paravertebral ganglia nine and ten of toads and frogs indicated neurochemical phenotype and cell size as markers of SPN phenotypes (Dodd and Horn, 1983; Lascar et al., 1996). There are two major types of neurons in these ganglia: secretomotor B and vasomotor C neurons. They noted that vasomotor C neurons expressed neuropeptide Y (**NPY**) and were 24% smaller in diameter than secretomotor B neurons that did not express NPY (Dodd and Horn, 1983). That the two types of neurons are of different functional subpopulations was further confirmed by varying inputs, axonal conduction velocities and membrane conductances. A more recent study of the mammalian superior cervical ganglion (**SCG**) showed SPNs of vasoconstrictor function were NPY^+ and were on average 20% smaller in diameter than SPNs of secretomotor function that were NPY^- (Headley et al., 2005). Additionally, they were innervated by PreSN fibers of different neurochemical profiles. Yet, these studies focus on certain ganglia lack data on the overall distribution of different SPN populations along the rostrocaudal axis.

Moreover, most previous studies on the SPNs have been done in rat, guinea pig, cat, frog, toad and embryonic chick models (Ernsberger and Rohrer, 1999). Mice SPNs are not often

studied, although mice are the accepted genetic mammalian models for studying a wide variety of structures, traits and diseases (Phifer-Rixey and Nachman, 2015). Mice are well understood, because they have been used in biomedical research since the beginning of the 20th century, and various genetic manipulations are possible. Additionally, they are biologically very similar to humans. Thus, understanding the SPN populations in the tPSG of mice is especially critical to future studies aimed at defining the mechanistic bases of plasticity associated with the emergence of autonomic dysreflexia after injury and disease states in humans.

In sum, as SPNs lying in different functional pathways can be distinguished by neurochemical/morphological criteria (Gibbins, 1992). I use such criteria to characterize the segmental distribution of tPSG noradrenergic and cholinergic neurons by comparing their numbers and size distributions in adult mice. This was important because we know nothing of this distribution, even though mouse is the most important genetic mammalian model, and yet the tPSG is a structure crucial to autonomic function and dysfunction.

I. Noradrenergic neurons

Most cell populations in the sympathetic chain have been identified as noradrenergic in all species studied (Muller et al., 1984), although the percentage of noradrenergic cells relative to the whole cell population within each ganglion varies amongst species and level. A study showed that 85-91% of the SPNs in the stellate ganglia of mice and 84-95% of SPNs in the stellate ganglia of rats were noradrenergic (Masliukov and Timmermans, 2004). Likewise, 89% of T4-T5 ganglia were found to be noradrenergic in guinea pigs (Gibbins, 1992).

The noradrenergic SPNs innervate a variety of targets, including the blood vessels, smooth muscles and nerve plexi of internal organs (Apostolova and Dechant, 2009). About 50% of noradrenergic SPNs are positive for NPY and serve a vasoconstrictor function in mice (Gibbins, 1991). The majority of PreSNs have vasoconstrictor function and synapse on the noradrenergic SPNs that innervate vasculatures throughout the body, from the head to the limbs (McLachlan, 2007). The blood vessels in the head and neck are supplied by sympathetic postganglionic fibers from the SCG, arms and upper part of the body from the stellate and upper thoracic ganglia, the abdominal visceral from coeliac and mesenteric and those in the lower part of the trunk and legs from lumbar ganglia (Burnstock, 1969).

Another innervation target of noradrenergic SPNs is the adrenal gland. In rats, a retrograde tracing study showed that 11.4% of neurons projecting to the adrenal gland in rats are from the SPNs, specifically from T5-T12, with 63% found within T7-T10 (Kesse et al., 1988). SPNs projecting to the adrenal gland were found in T1-T10 in guinea pigs, majority from T9-T10 (Parker et al., 1990). A study in mice has not been done.

II. Cholinergic neurons

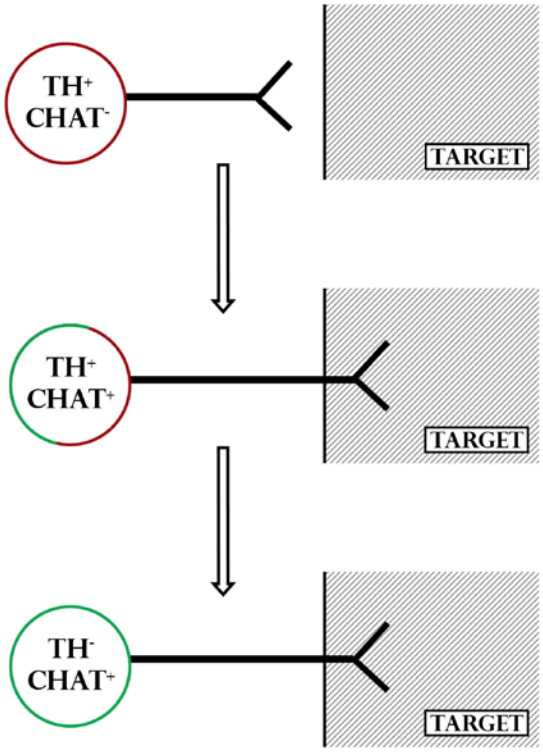

Figure 3. Schematic representation of target-dependent differentiation of cholinergic SPNs. The noradrenergic neurons express tyrosine hydroxylase (TH) (red), and the cholinergic neurons express choline acetyltransferase (ChAT) (green). The target tissue is represented as a gray box. The cholinergic SPN are differentiated from fully functional noradrenergic SPNs that do not express acetylcholine as they synapse on targets, including the sweat glands (Schafer et al., 1997). When the noradrenergic neurons form synapses on their targets, they stimulate the maturation of the target (Glebova and Ginty, 2005). Then, the targets secret factors that induce the cholinergic phenotype. There is a transient stage when these neurons exhibit both cholinergic and noradrenergic phenotypes, but they soon become fully cholinergic.

There are two hypotheses as to how the cholinergic SPNs develop: target-independent and target-dependent models. The target-independent model demonstrates a prenatal onset of the cholinergic phenotype during development. mRNAs for choline acetyltransferase (**ChAT**), an enzyme that synthesizes acetylcholine (Buckley et al., 1967), was detected as early as embryonic day 11 in mice, a day after the expression of tyrosine hydroxylase (**TH**), an enzyme that catalyzes early steps of catecholamine synthesis, reaches a significant level (Huber and Ernsberger, 2006). There are cholinergic SPNs that have been identified to be present in the primordial ganglia and are present in adulthood (Schafer et al., 1997; Morales et al., 1995). Cholinergic and noradrenergic co-phenotype has also been identified before innervation on

targets in transgenic mice (Schutz et al., 2008). The target-independent differentiation is not well-understood, and the factor regulating this early acquisition of cholinergic phenotype is unknown. The target-dependent model has been more elaborately studied and is the generally accepted model. Studies in the development of the cholinergic innervation of sweat glands and periosteum in rodents showed that the cholinergic phenotype develops postnatally as they receive factors that induce the cholinergic phenotype from their innervation target (Rao et al., 1994; Schafer et al., 1997; Asmus et al., 2000) (Figure 3). This model of cholinergic differentiation explains that the initially noradrenergic SPNs undergo a transient stage of expression of both adrenergic and cholinergic phenotypes and mature into cholinergic phenotype **(**Francis and Landis, 1999). Transplantation experiments (Schotzinger and Landis, 1988; Schotzinger and Landis, 1990; Schotzinger et al., 1994) and co-culture experiments (Habecker and Landis, 1994) on cholinergic innervation on sweat glands support this model. It is suggested that several cytokines, including ciliary neurotrophic factor – leukemia inhibitory factor, and cardiotophin 1 – act cooperatively to induce the switch (Apostolova and Dechant, 2009).

Many studies have quantified the percentages of SPNs in the PSG that are cholinergic. A number of these studies are listed in Table 1. This list demonstrates that only certain ganglia or the thoracic chain as a whole have been studied, and the composition of individual segments of tPSG remains unknown. Additionally, we can see that the percentages of SPNs are that cholinergic vary in different animal models and different levels of the chain. Cholinergic SPNs are also found in humans though the percentage has not been quantified (Weihe et al., 2005).

Table 1. A summary of experiments that quantified cholinergic populations within certain levels of the PSG. A clear discrepancy between species should be noted. The reason for this discrepancy is unknown. Note that Buckley et al. (1967) did not quantify the cholinergic population in terms of proportions.

Level	Animal model	Cholinergic neurons	Reference
Superior cervical	Cat	21.3%	Holmstedt and Sjoqvist (1959)
Superior cervical	Rat	<0.1%	Schafer et al. (1998)
Stellate (T1)	Cat	14.9%	Holmstedt and Sjoqvist (1959)
Stellate (T1)	Rat	5%	Schafer et al. (1998)
Stellate (T1)	Rat	3%	Masliukov and Timmermans (2004)
Stellate (T1)	Mouse	3%	Masliukov and Timmermans (2004)
Thoracic	Rat	In between 0.1-5%	Schafer et al. (1998)
L6	Cat	3.5%	Sjoqvist (1963)
L6	Cat	12.5%	Buckley et al. (1967)
L7	Cat	10.8%	Sjoqvist (1963)
L7	Cat	100 cells	Buckley et al. (1967)
S1	Cat	7.7%	Sjoqvist (1963)
S1	Cat	100 cells	Buckley et al. (1967)
S2	Cat	1.9%	Sjoqvist (1963)
Pelvic	Rat	0.5%	Keast et al. (1995)

Most studies on the function of cholinergic neurons in the PSG focus on the innervation of sweat glands in the skin (Landis and Fredieu, 1986; Schafer et al., 1997; Schafer et al., 1998;), although there have been studies on cholinergic innervation of the periosteum (Francis et al, 1997; Asmus et al., 2000). Cholinergic SPNs of caudal and rostral origins function in sweat control. Cholinergic cell bodies in the cat stellate ganglion and in the ganglia between L6 and S2 innervate the forelimb and give rise to cholinergic sweat secretory fibers (Sjoqvist, 1962; Sjoqvist 1963). In mice, it is hypothesized that eccrine sweat glands are found only on the footpads, where there are no hair follicles present (Taylor et al., 2012). It is highly likely that cholinergic SPNs with roles in sweat control are located in the levels near the footpads as do alpha motor neurons and noradrenergic neurons. In rats, forepaw sweat glands are innervated by cholinergic SPNs in the stellate ganglion and the hindpaw sweat glands by L4-L6 SPNs (Schafer et al., 1997; Dehal et al., 1992). In mice, the stellate ganglion is the known source of forepaw sweat glands (Schafer et al., 1998). Yet, contrary to this suggestion, the same study suggested that cholinergic SPNs caudal to the stellate ganglion were identified as the presumptive source of cholinergic sympathetic innervation of the hindpaw sweat glands, but the exact level was not identified.

III. An integrative approach

Noradrenergic systems can be identified with immunoreactivity towards TH (Ernsberger, 2000).

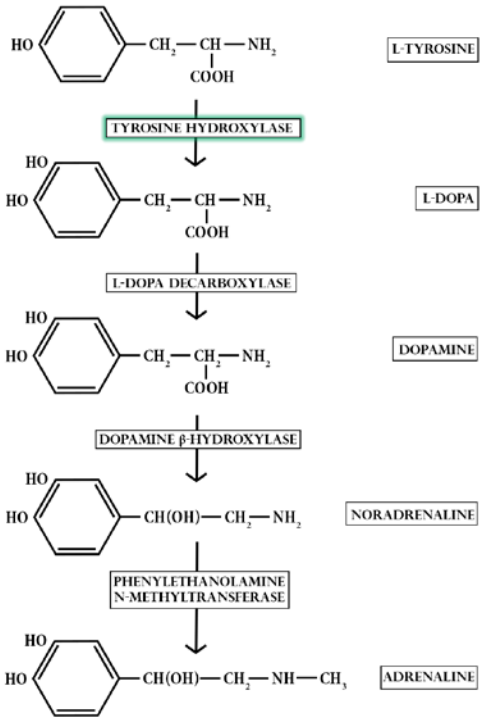

Figure 4. The catecholamine synthesis pathway. Tyrosine hydroxylase is the enzyme that initially converts L-tyrosine to L-DOPA. The enzyme that specifically synthesizes noradrenaline from dopamine is dopamine beta-hydroxylase (DBH). Noradrenaline can be further differentiated into adrenaline by phenylethanolamine n-methyltransferase.

The initial step of the catecholamine synthesis pathway (detailed in Figure 4) involves TH, which catalyzes the conversion of L-tyrosine to L-DOPA, a precursor to dopamine, noradrenaline, and adrenaline (Nagatsu et al., 1964; Goodall and Kirshner, 1958). Thus, an SPN containing TH could be dopaminergic, noradrenergic, or adrenergic (Nagatsu et al., 1964; Semenenko et al., 1986). Dog stellate ganglia incubated either with tyrosine and L-dopa synthesized dopamine and norepinephrine, and "questionable amounts" of epinephrine of little importance to the sympathetic function (Goodall and Kirshner, 1958). Yet, Teitelman et al. (1979) found that cells containing TH and dopamine beta-hydroxylase (**DBH**), the final enzyme

of noradrenaline synthesis, in the primordial of the thoracic ganglia never stained for one enzyme but not for the other. TH and DBH appear simultaneously at E11. Thus, the catecholamine contained in the sympathoblasts in the sympathetic chain is most probably not dopamine . The cells in the sympathetic ganglion were always negative for phenylethanolamine n-methyltransferase, which converts noradrenaline to adrenaline (Teitelman et al., 1984). Thus, Teitelman confirmed that TH^+ SPNs were noradrenergic, and our experiment is based on the assumption that this is true. Yet, we cannot disregard the possibility of the presence of catecholaminergic neurons that are dopaminergic or adrenergic and were not yet identified, and subsequent studies need to need to be done using other synthesis enzymes in the noradrenaline synthesis pathway (Klimaschewski et al., 1996).

Cholinergic cells can also be identified using immunohistochemistry by testing for immunoreactivity towards ChAT (Buckley et al., 1967).

Another method to fluorescently identify the cholinergic and noradrenergic systems is creating a transgenic mouse line expressing fluorescent protein under control of the promoter associated with the gene of interest (Srivastava and Ow, 2015). For example, to identify cholinergic cells, we can use a line expressing enhanced green fluorescent protein (**eGFP**) under control of the promoter for ChAT. When the gene of interest is expressed under that specific promoter, the fluorescent protein will also be expressed to allow for direct visualization using epifluoresence (e.g. GFP) and it is possible to have its fluorescence further amplified with antibodies raised against the protein (e.g. anti-GFP).

We used immunohistochemistry to identify noradrenergic SPNs within the tPSG, and a transgenic mouse line in combination with immunohistochemistry to identify cholinergic SPNs.

METHODS

Ethical Approval

All experimental procedures to be described comply with the principles of "The Guide for the Care and Use of Laboratory Animals" outlined by the American Physiological Society. We abide by the protocols outlined by the Emory University Institutional Animal Care and Use Committee (IACUC).

Tissue preparation

Two ChAT-eGFP mice (JAX:007902) were sacrificed by perfusion fixation at P91 and P101 respectively. They were anesthetized in an isofluorane chamber and injected with 40mg/kg urethane, intraperitoneally. The mice were then transcardially perfused through the ventricular catheter with saline and fixatives. The tissues were fixed in 4% paraformaldehyde overnight and transferred to a 15% sucrose solution and stored at 4°C. The tPSG (stellate-T13) were isolated and immersed in 15% sucrose for cryopreservation.

Cryostat sectioning

The isolated tissue was mounted on a frozen cryostat chuck using TissueTek® optimal cutting temperature compound. The chuck was left on dry ice for the tissue to freeze and placed in the cryostat at ~-21°C. The thickness of the sections was adjusted to 8 µm. Fisherbrand's superfrost/plus microscope slides were used to collect sectioned tissue. To avoid sampling errors, we counted SPNs on every section we obtained.

Fluorescence immunohistochemistry

The slides were hydrated in phosphate buffered saline (PBS) for an hour and permeabilized with PBS containing 0.3% Triton X-100 (0.3% PBS-T) overnight. Subsequently, the sections were incubated for 2-3 days with the primary antibodies (Table 2). The preparations were then washed in 0.3% PBS-T (3X, 30 minutes), before incubating at 4°C with the secondary antibodies for 1.5 hours in room temperature (Table 3). The slides were left to dry after a final wash in PBS-T (20 minutes) and 50mM Tris-HCl (2X 20 minutes). They were then coverslipped with SlowFade® Gold antifade reagent with diamidino-2-phenylindole (DAPI).

Table 2. Primary antibodies used for immunohistochemistry (TH*:* tyrosine hydroxylase; GFP: green fluorescent protein). The tissues were incubated in these antibodies for 2-3 days at 4°C.

Primary	Host species	Dilution	Source
TH	Sheep	1:100	Millipore
GFP	Chicken	1:100	Jackson

Table 3. Secondary antibodies used for immunohistochemistry (Cy3: Cyanine 3). The sections were incubated in these antibodies for 1.5 hours at room temperature.

Secondary and streptavidin complex	Dilution	Source
Cy™3 donkey pAB to GFP anti-sheep IgG	1:250	Abcam
Alexa Fluor® 488-conjugated Affinipure donkey anti-chicken IgY(IgG)	1:100	Abcam

Image analysis: counting cells and estimating cell diameters

Figure 5A provides an example of the fluorescent labeling observed. The sections were analyzed under Olympus BX51. Neurolucida neuron tracing and counting software (MBF Bioscience) was used to trace the cell bodies (Figure 5B). The cell bodies were selected based on whether they were positive for ChAT and/or TH and whether their nuclei were present, as confirmed by DAPI staining to avoid redundant counting of the same cell body in different sections. Neurolucida Explorer was used to obtain the maximum and minimum feret values for each tracing. The cell diameter was calculated by averaging the two values.

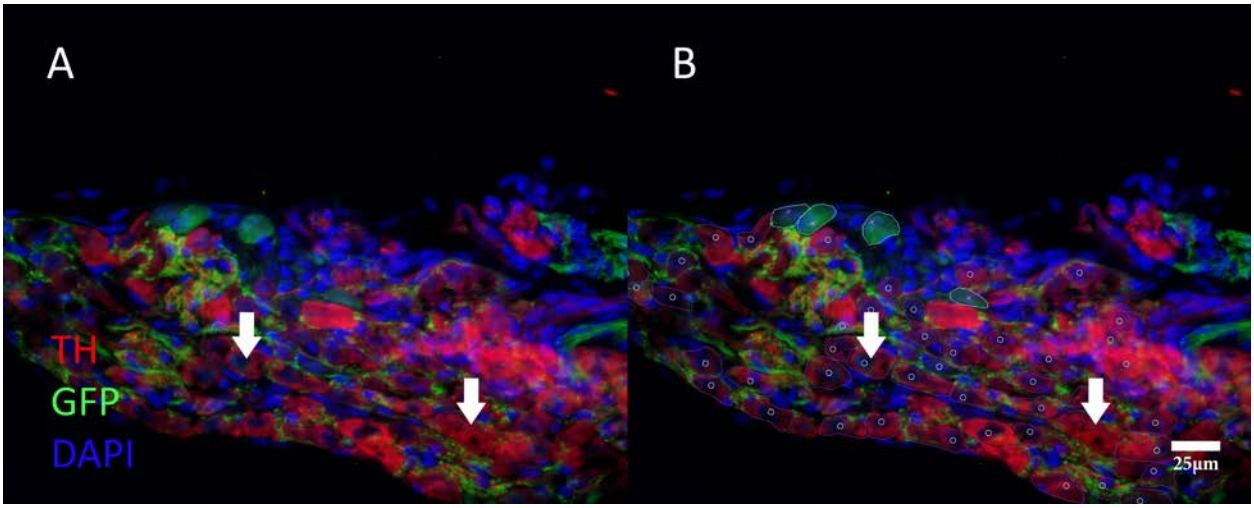

Figure 5. An 8µm section of a T2 ganglion of a CG mouse immunostained for TH (red), GFP (green), and DAPI (blue) to identify TH^+ and $ChAT^+$ populations. The photos were taken using Nikon E800. A) The majority of the SPNs express TH, shown in red. PreSN fibers forming basket-like synapses around the SPNs as well as a small population of SPNs express ChAT, shown in green. The $ChAT^+$ neurons were often in clusters as shown. All cell nuclei, including glial nuclei, are stained blue with DAPI, which binds to DNA in the nuclei of all cells, not specific to neurons (Loesel et al., 2006). We counted SPNs that were either TH^+ or $ChAT^+$ and contained nuclei. The right arrow indicates a TH^+ SPN without a nucleus and the right arrow indicates a TH^+ SPN with a nucleus. Only the cell body with a nucleus, as the soma on the left does, was traced. B) An example of cell body outlines traced using Neurolucida. This image shows the tracings used for a computation of the cell diameters. TH^+ cell bodies were traced in pink, with their nuclei marked with circles, and $ChAT^+$ cell bodies were traced in cyan, with their nuclei marked with X's (40x; Scale bar = 25µm).

Statistical analysis

Three statistical analyses were performed: 1) paired student's t-test, 2) unpaired student's t-test and (3) analysis of variance (ANOVA). The t-tests were executed on Microsoft Excel, and the ANOVA was conducted using SPSS Statistics software.

RESULTS

I. Identifying cholinergic and noradrenergic populations

We observed four distinct neurochemical phenotypes among the SPNs in the tPSG: $TH^+/ChAT^-$ SPNs, $TH^-/ChAT^+$ SPNs, $TH^+/ChAT^+$ double-labeled SPNs, and $TH^-/ChAT^-$ SPNs (Table 4). The primary population of $TH^+/ChAT^-$ SPNs was considered noradrenergic, although TH is only the initial step of catecholamine synthesis, not a specific marker for noradrenergic neurons, for reasons described in the introduction.

The $TH^-/ChAT^+$ SPNs and $TH^+/ChAT^+$ double-labeled SPNs were all considered cholinergic neurons. The $TH^+/ChAT^+$ SPNs were considered late-maturing cholinergic SPNs going through the affinitive switch described in the introduction. A sample of ten sections of a T2 ganglion showed that there was at most one double-labeled SPN per section.

The $TH^-/ChAT^-$ population was disregarded in this study. Their nuclei were stained with DAPI, but their somas were not positive for TH or ChAT. A sample of ten sections of a T2 ganglion showed that there were 2.4±0.3 $TH^-/ChAT^-$ SPNs per section. Although there have been studies that showed that cholinergic and noradrenergic populations do not add up to 100% of the SPN population (81-91% of the mouse ganglionic population is noradrenergic and 3% is cholinergic, Masliukov and Timmermans, 2004), no previous study has been done on the functional significance of $TH^-/ChAT^-$ SPNs. Since the purpose of our study was to specifically characterize cholinergic and noradrenergic SPNs, they were disregarded.

Table 4. A summary of the four phenotypes of the SPNs observed in the tPSG. Their immunoreactivity for TH and GFP, as well as nuclear staining for DAPI have been recorded. Our interpretation of each population is summarized in the last column. In short, $TH^+/ChAT^+$ SPNs were recorded as noradrenergic neurons and $TH^-/ChAT^+$ as well as $TH^+/ChAT^+$ neurons were viewed as cholinergic neurons.

Phenotype	TH	GFP (ChAT)	DAPI	Interpretation

$TH^+/ChAT^-$	+	-	+	Noradrenergic
$TH^-/ChAT^+$	-	+	+	Cholinergic
$TH^+/ChAT^+$	+	+	+	Cholinergic
$TH^-/ChAT^-$	-	-	+	Disregarded

II. Noradrenergic vs. cholinergic SPNs

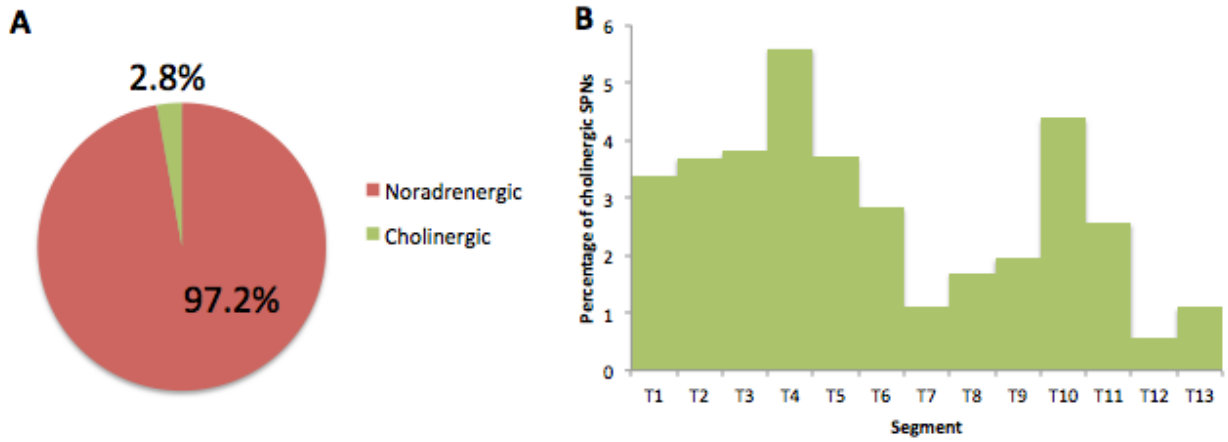

Figure 6. A) The pie chart depicts the percentages of noradrenergic SPNs (red) and the cholinergic SPNs (green) relative to all SPNs investigated in the 12 segments of thoracic chain in two animals. We counted 25,480 noradrenergic SPNs, which comprised 97.2% of all SPNs observed, and 735 cholinergic SPNs which comprised 2.8%. A) Shown are the mean percentages of neurons that are cholinergic relative to the SPN population in each ganglion of the two mice. T12 ganglion was studied only in mouse #1 and T13 only in mouse #2 and thus are not average percentages. The percentages of cholinergic SPNs relative to the full ganglionic population range from 0.6 to 5.6%. There are significantly more cholinergic neurons in the rostral segments (496 in T1-T6) than the caudal segments (239 in T8-13), although T10 is has a higher percentage of cholinergic neurons than most of the rostral segments (unpaired t-test; $p < 0.05$).

The total count of SPNs in T1-T13 of two mice was 26,215. As expected, the majority of the SPNs were noradrenergic as shown in Figure 6A, with the remainder being cholinergic. The cholinergic population comprised 0.6-5.6% of the ganglionic population in each level of the thoracic chain (Figure 6B). The rostral segments (T1-T6) had a significantly higher percentage of cholinergic neurons compared to the caudal segments (T7-T13) ($p < 0.05$).

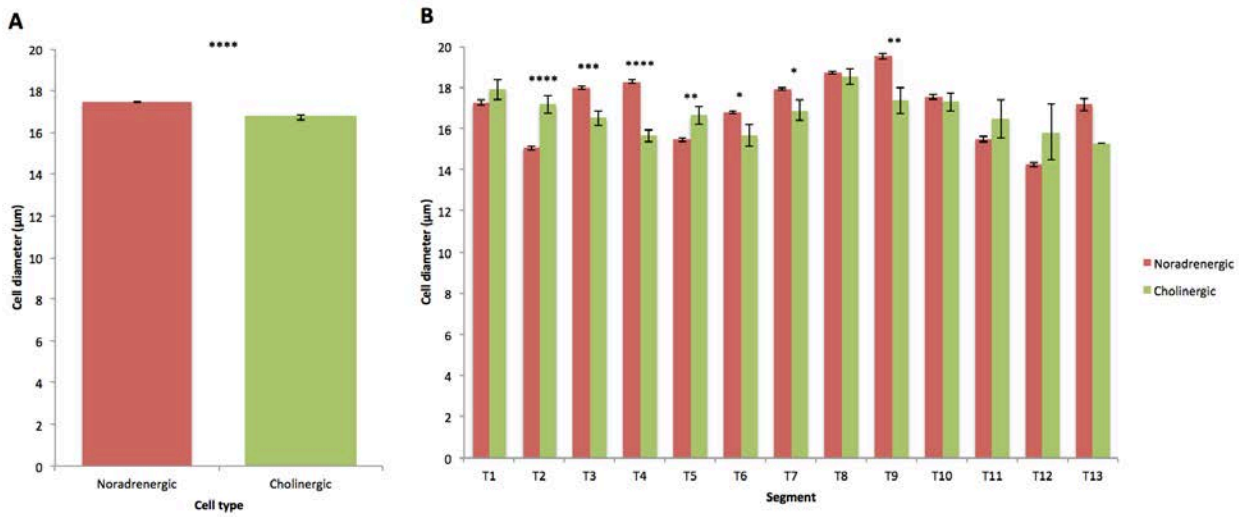

Figure 7. A comparison of noradrenergic and cholinergic SPN diameters in the tPSG (n = 2). A) The average cell diameter of 25,778 noradrenergic neurons was 17.47±0.03µm and of 735 cholinergic neurons was 16.73±0.14µm. There was a significant difference in the diameters of all noradrenergic SPNs and the diameters of all cholinergic SPNs (unpaired heteroscedastic t-test; $p<0.0001$). B) A graph of the average diameters of noradrenergic and cholinergic SPNs in each segmental level. One type of neuron is not consistently bigger or smaller in all levels of the chain. The noradrenergic neurons are larger in T3-T4, T6-T10 and T13, and the cholinergic neurons are larger in T1-T2, T5, and T11-T12. The diameters were significantly different in T2-T7 and T9 (unpaired heteroscedastic t-test; $p<0.05$ *, $p<0.01$**, $p<0.001$***, and $p<0.0001$ ****). T1 and more caudal T8, T10-T12 noradrenergic and cholinergic populations did not have a significant difference in their diameters. T13 could not be statistically analyzed, because there was only one cholinergic SPN. The diameters of both types of neurons do not constantly increase/decrease along the rostrocaudal axis. The increase/decrease in the average diameters in consecutive levels no more than 2.92µm. Bar graphs show data as mean±standard error.

Figure 7 shows a comparison of noradrenergic and cholinergic SPN diameters. The average cell diameter was 17.47±0.03µm for noradrenergic neurons and 16.73±0.14µm for cholinergic neurons as shown in Figure 7A. A comparison of the mean values of the diameters showed a significant difference between the two values. Figure 7B shows the average cell diameter of noradrenergic and cholinergic SPNs in each thoracic ganglion. The diameters are not significantly different in all levels of the thoracic ganglia. Additionally, the noradrenergic neurons are not consistently larger than cholinergic neurons and vice versa. In each level of the tPSG, either type of neuron can be larger or smaller, and there is no distinct pattern of increase/decrease in cell diameter in either type of neuron.

III. Intraspecies variations

Table 5. Information regarding the two ChAT-eGFP mice studied. Compared in this table are their sex, postnatal age at sacrifice, levels of the PSG isolated, and the total number of neurons found in 12 ganglia of each mouse. They had parents that were littermates i.e., the two fathers were littermates and the two mothers were littermates. One is a female mouse and one is a male mouse. Although their sexes differ, they were both sacrificed about 3 months after birth and both had 12 levels of the thoracic segment isolated. Despite the similarities between the two mice, there is a 3-fold difference in the total number of SPNs found in the tPSG of these mice.

Animal	#1	#2
Sex	Female	Male
Age at sacrifice	101	91
PSG isolated	T1-T12	T1-T11, T13
Total number of neurons	6,494	19,721

Table 5 compares the two ChAT-eGFP we studied. The two mice are labeled #1 and #2 for convenience. They were genetically related in that they had mothers who were littermates and fathers who were also littermates. They were fixed at P91 and P101, and 12 levels of the thoracic ganglia were isolated from each mouse. A notable difference was that one mouse was male and the other was female. We observed highly variable results from the two mice. There was a 3-fold difference in the number of the observed SPNs as shown in Table 5. Both the distribution and size of each of noradrenergic and cholinergic populations also differed between these two subjects and will be described in the subsequent sections of this paper.

Observing considerable individual differences, we integrated counts from individual ganglia in 6 additional mice to seek for a possible factor that could be contributing to the difference. Table 6 and Figure 8 summarize the information on the 8 mice and the results we found regarding the number of SPNs and their diameters. It was difficult to find a pattern in the variation in this sample. Yet, this comparison showed that we cannot attribute the differences in our sample to sex differences. The diameters in different animals differed significantly in all ganglia ($p<0.0001$ in all ganglia).

Table 6. The sum of noradrenergic and cholinergic SPNs and the mean ± standard error values of these SPNs in the T3, T5, and T9 ganglia of 8 subjects are shown. Mice #3-8 were either spinalized at T2-3 or surgical sham controls as noted in the spinalization column. Mice #3, 4, 7, 8 were female and 5 and 6 were male. Mice #7 and 8 were ChAT-GSAT-GM24-cre::tdTomato (CTd) mice, different from the ChAT-eGFP (CG) mice we used in this study. Every fifth section obtained was looked at in animals 5-8; consequently total cell number was estimated following multiplication by 5. Yet, the average number of SPNs was still smaller than observed in the mice where all sections were looked at (#1-4) overall and also in each ganglion.

Ganglion	Animal #	Strain	Sex	Age at sacrifice	Spinalization	# of SPNs	Cell diameter (µm)
T3	1	CG	F	101	Control	2,683	18.0±0.1
	2	CG	M	91	Control	2,443	18.6±0.1
	3	CG	F	41	Sham	975	13.2±0.1
	4	CG	F	41	Spinalized	1,646	15.2±0.8
T5	1	CG	F	101	Control	939	13.0±0.1
	2	CG	M	91	Control	1,088	17.6±0.1
	5	CG	M	71	Sham	260	23.0±0.8
	6	CG	M	68	Spinalized	210	22.6±0.5
T9	1	CG	F	101	Control	413	12.4±0.2
	2	CG	M	91	Control	1,688	21.2±0.1
	7	CTd	F	97	Sham	280	22.5±0.7
	8	CTd	F	97	Spinalized	320	19.2±0.5

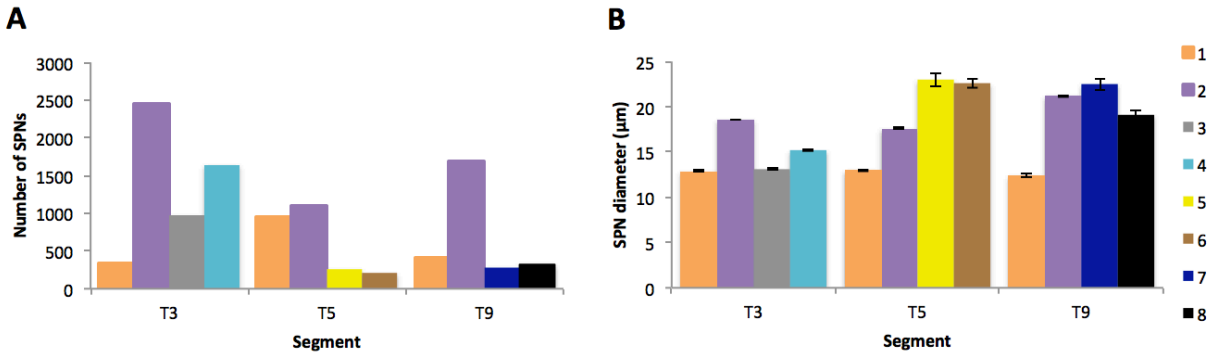

Figure 8. A) A graphical representation of the number of SPNs and their cell diameters shown Table 6. There is no distinct identifiable trend specific to segmental differences or any of the characteristics in these mice listed in the first six columns of Table 6. Because there was more than one known factor attributing to the difference in the 8 subjects, and possible additional unknown factors, it was difficult to determine which factor is responsible for which variation. B) The average diameter of SPNs in each animal in T3, T5 and T9. The diameters in different animals differed from one another in all ganglia, but there was no significant trend that could be extrapolated form this difference (T3: ANOVA, $F(3,7743) = 710.196$, $p < 0.0001$; T5: ANOVA, $F(3,2217) = 385.554$, $p < 0.0001$; T9 ANOVA, $F(3,2217) = 447.585$, $p < 0.0001$)

I. Noradrenergic neurons

Noradrenergic neurons comprised 94.4-99.4% of the SPNs residing in each ganglion. There were as few as 90 to as many as 3,933 TH^+ SPNs in an individual ganglion of the thoracic chain in our sample. Figure 9A shows the segmental distribution of noradrenergic neurons in both mice. The middle segments (T3-T8) have more TH^+ labeled SPNs compared to the either ends of the chain. There were 19,025 SPNs in subject #2 compared to 6,455 in subject #1, and thus 9A is dominated by the distribution obtained from the second subject rather than both mice equally. Figure 9B compares the segmental distributions of TH^+ SPNs between the two mice throughout the thoracic levels of the chain. The two mice show very different distribution patterns. The second subject's noradrenergic population peaks are T7 and T8 as in Figure 9A. In contrast, T7 and T8 are the smallest in the first subject along with T10, and the distribution peaks at T2 and T12.

Table 7. The number of noradrenergic SPNs per ganglion, the proportion of each ganglionic noradrenergic SPNs relative to all ganglionic noradrenergic SPNs, and the mean noradrenergic SPN diameters in each segment in 13 different levels of ganglion from two animal are shown. An exception is in the T3 ganglion, where two additional animals have been studied. The proportion is not shown in these two animals, because only one ganglion was studied. The cell diameters are denoted mean±standard error of 13 different levels of ganglia from # subjects.

Level	Animal	Number of noradrenergic SPNs	Proportion relative to all noradrenergic SPNs (%)	Average cell diameter (μm)
T1	#1	599	9.3	15.2±0.2
	#2	598	3.1	19.3±0.2
T2	#1	1107	17.1	13.3±0.1
	#2	534	2.8	18.7±0.2
T3	#1	338	5.2	12.9±0.2
	#2	2341	12.3	18.7±0.1
	#3	931		13.3±0.1
	#4	1531		15.3±0.1
T4	#1	327	5.1	13.4±0.2
	#2	2153	11.3	19.0±0.1
T5	#1	934	14.5	13.1±0.1
	#2	1018	5.4	17.7±0.1
T6	#1	490	7.6	13.3±0.2
	#2	1671	8.8	17.8±0.1
T7	#1	250	3.9	10.5±0.2
	#2	3933	20.7	18.4±0.1
T8	#1	285	4.4	13.4±0.2
	#2	3766	19.8	19.1±0.1
T9	#1	411	6.4	12.4±0.2
	#2	1649	8.7	21.3±0.1
T10	#1	113	1.8	13.6±0.3
	#2	1110	5.8	18.0±0.1
T11	#1	522	8.1	14.7±0.2
	#2	162	0.9	18.0±0.3
T12	#1	1079	16.7	14.3±0.1
T13	#2	90	0.5	17.2±0.3

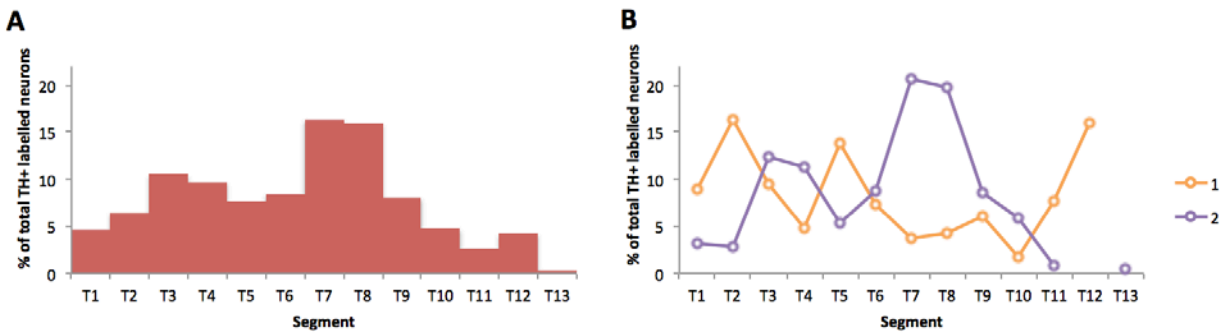

Figure 9. A) The distribution of 25,480 TH^+ noradrenergic cell bodies throughout the tPSG (T1-T11 n=2; T12-T13 n=1). The graph shows the percentages of noradrenergic SPNs within each ganglion compared to the total number of noradrenergic SPNs in the thoracic ganglia. The middle segments (T3-T8) have more TH^+ labeled SPNs compared to the very rostral (T1-T2) and caudal (T9-T13) segments. Because subject #2 has more TH^+ SPNs (19025) compared to subject #1 (6455), the distribution in A) is dominated by the second subject as shown in purple in B. This is true is all part A's of subsequent figures in the results section. B) This graph shows the distribution of TH^+ SPNs in the two subjects separately. Note that the subject #1's SPN distribution (orange) peaks at either ends (T2 and T12) whereas the second subject's distribution (purple) peaks in the middle thoracic region (T7 and T8). The male and female distributions are significantly different (paired t-test, $p<0.05$, T1-T11). The points missing in B) (T12 in male and T13 in female) indicate that these ganglia were not studied. This will hold true in all graphs from here on.

Figure 10 describes the noradrenergic SPN diameters in each level of the tPSG. Figure 10A is based on a compilation data on the noradrenergic SPNs found in both subjects. The mean diameters of SPNs in the different levels of the thoracic chain were statistically significantly different from one another (ANOVA, $F(12,24959) = 254.882$, $p < 0.0001$), although a distinct pattern of increase/decrease along the rostrocaudal axis cannot be observed. Additionally, the average diameters of the two mice were significantly different as shown in Figure 10B (paired t-test, $p < 0.0001$, T1-T11). Subject #1 has significantly larger average noradrenergic SPN diameter values compared to subject #2.

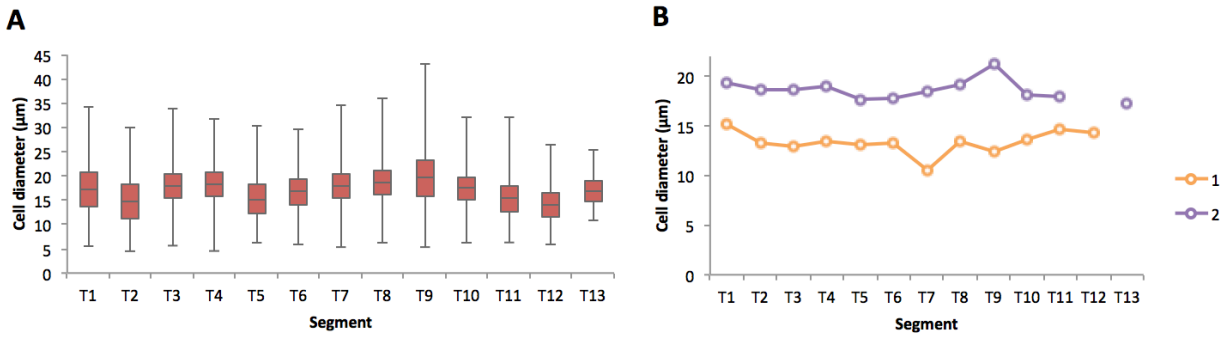

Figure 10. A) A boxplot of the diameters of noradrenergic SPNs in each level of the tPSG. (T1-T11 n=2; T12-T13 n=1). The error bars indicate the maximum and minimum values. The box is limited by 1st and 3rd quartiles. The median is indicated by the vertical line that runs through the center of the box. The differences among the mean values were shown to be statistically significantly different (ANOVA, $F(12,24959) = 254.882$, $p < 0.0001$). B) Observing the data from each sample separately, we observed that the average diameters do not fluctuate among different segments, but the two subjects' SPN average diameters differ significantly on all levels, T1-T11 (paired t-test, $p<0.05$). The average cell diameter of subject #1 was 13.3µm and for subject #2 was 18.6µm.

II. Cholinergic neurons

Cholinergic SPNs comprised 0.6-5.6% of all SPNs in each tPSG. Figure 11A shows the segmental distribution of cholinergic neurons in both mice. There are significantly more cholinergic neurons in the rostral ganglia (T1-T6) (496) than the caudal ganglia (T7-T13) (239) (unpaired t-test, $p < 0.05$). As with Figure 9A, this distribution is dominated by values obtained in the second subject, due to its larger sample size of SPNs. Yet, the pattern of more rostral SPNs compared to caudal SPNs seems to hold true also in the first subject (Figure 11B).

Table 8. The number of cholinergic SPNs per ganglion, the proportion of each ganglionic cholinergic SPNs relative to all ganglionic cholinergic SPNs, and the mean cholinergic SPN diameters in each segment in 13 different levels of ganglion from two animal are shown. An exception is in the T3 ganglion, where two additional animals have been studied. The proportion is not shown in these two animals, because only the T3 ganglion was studied. The cell diameters are denoted mean±standard error of 13 different levels of ganglia from # subjects. The missing average cell diameter entries denote that the ganglion did not contain any cholinergic SPNs. In ganglia containing only one cholinergic SPN, the standard error values are omitted.

Level	Animal	Number of cholinergic SPNs	Proportion relative to all cholinergic SPNs (%)	Average cell diameter (μm)
T1	#1	3	9.4	13.6±1.9
	#2	39	5.6	18.2±0.5
T2	#1	6	18.8	13.0±1.0
	#2	57	8.2	17.6±0.4
T3	#1	4	12.5	12.2±2.4
	#2	102	14.7	16.7±0.4
	#3	44		10.7±0.5
	#4	115		15.3±0.3
T4	#1	0	0	
	#2	147	21.2	15.7±0.3
T5	#1	5	15.6	12.2±1.9
	#2	70	10.1	16.9±0.4
T6	#1	10	31.3	13.1±0.9
	#2	53	7.6	16.1±0.6
T7	#1	1	3.1	16.2
	#2	46	6.6	16.9±0.5
T8	#1	1	3.1	16.4
	#2	69	9.9	18.6±0.4
T9	#1	2	6.3	13.6±0.7
	#2	39	5.6	17.6±0.7
T10	#1	0	0	
	#2	56	8.0	17.3±0.4
T11	#1	1	3.1	13.9
	#2	17	2.4	16.6±1.0
T12	#1	6	3.1	15.9±1.4
T13	#2	1	0.1	15.3

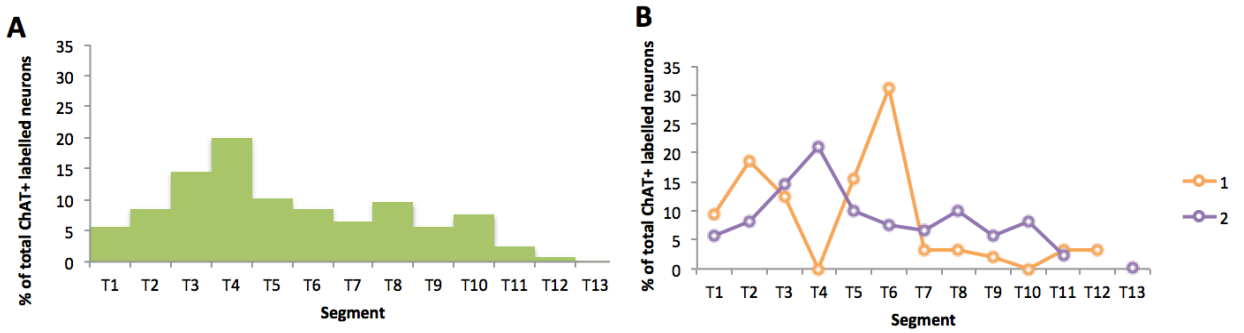

Figure 11. A) The distribution of 735 ChAT$^+$ cholinergic cell bodies throughout the tPSG (T1-T11 n=2; T12, T13 n =1). The graph shows percentages of ChAT$^+$ labeled SPNs within each ganglion compared to ChAT$^+$ SPNs in all thoracic ganglia. As previously discussed in Figure 6, the rostral segments (T1-T6) have more ChAT$^+$ labeled SPNs (496) compared to the caudal (T7-T13) segments (239) (unpaired t-test; $p < 0.05$). B) This graph shows the distribution of ChAT$^+$ SPNs in the two subjects separately. The distributions are significantly different in all ganglia, T1-T11 (unpaired t-test, $p<0.001$)

Cell diameters of ChAT$^+$ cholinergic neurons are shown in Figure 12. The mean diameters of SPNs of different segmental origin were statistically significantly different (ANOVA, $F(12,722) = 3.829$, $p<0.0001$). Again, a trend of increase or decrease in cell diameter cannot be observed along the rostrocaudal axis. As with noradrenergic SPNs, the cholinergic SPN diameters are significantly larger in the second subject than the first subject as shown in Figure 12B (paired t-test, $p<0.01$, T1-T11).

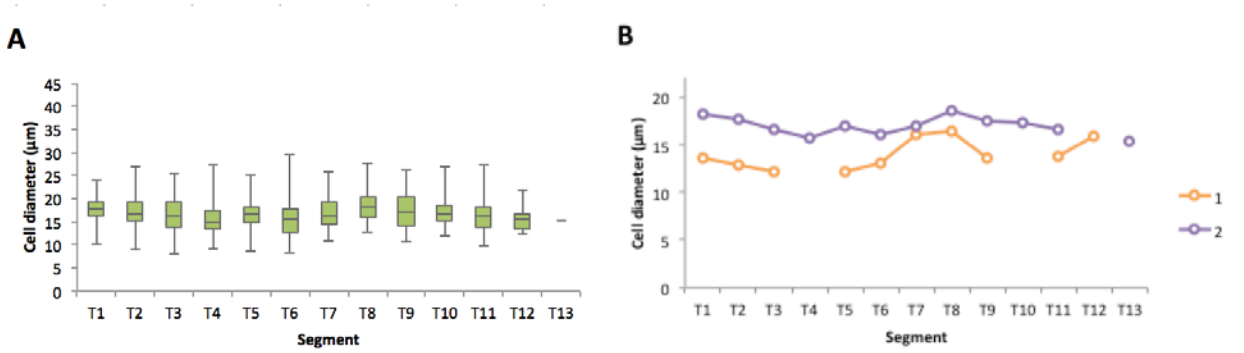

Figure 12. A) A boxplot of the ChAT$^+$ SPN diameters for each tPSG (T1-T3, T5-T9, T11 n=2; other levels n =1) The maximum and minimum values are indicated with the error bars. The box is limited by 1st and 3rd quartiles, and the median value is indicated by the vertical line that runs through the center. The differences among the mean values were shown to be statistically significantly different (ANOVA, $F(12,722) = 3.829$, $p < 0.0001$). Note that T13 had only one sample. B) Observing the data from each sample separately, we can see that there are differences in the ChAT$^+$ SPN diameters of the two mice that were examined. The average cell diameter in all ganglia was 14µm in subject #1 and 17µm in subject #2. Consistent with A), the diameters are significantly different among the ganglia (paired t-test, $p<0.0001$, T1-T11).

DISCUSSION

Segmental differences in the number and diameters of noradrenergic and cholinergic SPN populations residing in the tPSG were studied. This is the first study that characterized noradrenergic and cholinergic SPN distribution and cell diameter on every level of the thoracic chain. Through this study, we obtained insight into the relative segmental numbers of cholinergic and noradrenergic neurons as well as the enormous inter-animal heterogeneity in numbers seen. Observations provide an important reference sample for consideration when additional characterizations in tPSG properties are undertaken in mouse, including in relation to changes observed in development, after injury, or in disease.

As previously observed, the majority of the SPNs, 97.2%, in the tPSG were noradrenergic neurons (Elfvin et al., 1993). The percentage of noradrenergic SPNs in T4-T6 (95.9%) was comparable to an earlier study (88.4%) of three mice (Jobling and Gibbins, 1999). However, it should be noted that they only looked at one midsection of the ganglia, whereas we looked at all sections. The numbers noted in this study in mice are not consistent with the numbers found in guinea pig (Lichtman et al, 1980). Compared to 24,675 cells in the stellate ganglion and 1,575 in the T5 they found, we found on average 598.5 in the stellate ganglion and 976 in T5. Differences are explained by body size difference in the two species, as Purves et al. (1985) found that there were more cervical ganglion cells in species of higher body weight.

We observed that the number of noradrenergic populations per ganglion peaked at T7 and T8. For reference, the noradrenergic fibers innervating the adrenal gland were found to be located from T5-T12 ganglia (Kesse et al., 1988). In addition to the noradrenergic SPNs that innervate the vasculature throughout the body distributed along the length of the chain, these

SPNs concentrated in the T7-T8 ganglia could be of greater quantity compared to other ganglia due to the presence of additional SPNs that innervate the adrenal gland.

The remainders were cholinergic neurons that comprised only 2.8% of the whole thoracic SPN population. Regarding percentages, 0.6 to 5.60% of the SPNs in each thoracic ganglion were cholinergic, consistent with 0.1-5% observed by Schafer et al. (1998) in rat thoracic ganglia and 3% observed in stellate ganglion of rats and mice by Masliukov and Timmermans (2004). There were more cholinergic neurons in the rostral segments (T1-T6) than in the caudal segments. A large population of T1-T6 noradrenergic neurons innervate vasculature in the rostral part of the body. In comparison, most cholinergic neurons in the PSG innervate sweat glands in the skin, although there have been studies on cholinergic innervation of limb arteries and the periosteum (Landis and Fredieu, 1986; Schafer et al., 1997; Schafer et al., 1998; Asmus et al., 2000). In mice as in rats and cats, sweat glands are present only in the footpads where there are no hair follicles (Mustonen et al., 2003; Taylor et al., 2012). Mice have eccrine sweat glands in their footpads and no apocrine sweat gland, which are connected to hair follicles (Scrivener and Cribier, 2002). Their sweat glands do not serve any thermoregulatory function as do in humans (Janig and Habler, 2003). They secrete sweat to increase traction for improved mobility (Stumpf et al., 2004). The limited number of sweat glands in mice could be the reason for the small cholinergic population in the tPSG we observed. It is known that cholinergic innervation on the footpad sweat glands come from noradrenergic SPNs that differentiated into cholinergic SPNs (Landis and Keefe, 1983). However, the exact segmental location of the innervating SPNs within the PSG is unclear.

There is differential distribution in the thoracic segment and their innervating target tissue; the sympathetic ganglia are subdivided into regions of neurons that innervate specific

peripheral tissue (Lindh et al., 1986b). The ganglia in each region have different chemical and functional properties. The stellate ganglion is the known source of forepaw sweat glands. The cholinergic SPNs caudal to the stellate ganglion were identified as the presumptive source of cholinergic sympathetic innervation of the hindpaw sweat glands (Schafer et al., 1998). Yet, the exact segment of the tPSG has not yet been identified. According to our data, the upper thoracic segments could be the origin of additional cholinergic fibers that innervate forepaw in mice. It is unlikely these neurons innervate mouse hindpaw since in rats this originates from L4-L6 SPNs (Dehal et al., 1992).

Most SPNs in the PSG have been previously found to be 15-35μm (Smolen, 1988). Our results are consistent with this finding, except we also found smaller SPNs (5μm-15μm). The average diameters of noradrenergic and cholinergic SPNs were 17.5 μm and 16.7 μm, respectively. There have been previous studies that found two types of neurons of different sizes. In addition to the studies mentioned in the introduction, Masliukov and Timmermans (2004) found that mice had TH^+ neurons of 360μm^2 cross-sectional area $ChAT^+$ neurons of 480μm^2 in the stellate ganglion, which we can translate into 21.4μm and 24.5μm diameters. They reported that $ChAT^+$ neurons were significantly larger in comparison to TH^+ neurons in the superior cervical ganglion in mice. Our results are not consistent with this study, since we found that there is no significant difference in the sizes of TH^+ and $ChAT^+$ neurons in T1, but we observed a slightly larger cholinergic SPN diameter than noradrenergic SPN diameter at T1. Another study in T4-T6 of mice showed noted that noradrenergic SPNs have an average cross-sectional area of 533±15μm^2 (i.e. 34.0μm diameter), which is larger than 13.0μm diameter of noradrenergic SPNs found in our study. Yet, as we did at those levels, they noted that the noradrenergic SPNs are "significantly larger than other neurons" in the ganglia (Jobling and Gibbins, 1999). Honma

(1970) also observed a bimodal distribution of cell sizes of the 10th sympathetic ganglion of the toad: 34 and 43μm peaks. Hill and Burnstock (1975) suggested that different sizes of these neurons represented different stages in development or represented functionally distinct neurons – smaller still in the process of differentiation. We could hypothesize that the size discrepancy arises from the fact the cholinergic differentiation is delayed compared to the noradrenergic differentiation (Huber and Ernsberger, 2006). Noradrenergic phenotype is expressed in sympathetic neuroblasts as early as E9-10 in mice (Pattyn et al., 1999). According to the target-independent model of cholinergic differentiation, the cholinergic neurons develop postnatally (Schafer et al., 1997). The target-dependent model also supports that the cholinergic differentiation is delayed. In mice, the earliest detection of mRNAs for ChAT was detected was E11, a day after the expression of TH reaches a significant level (Huber and Ernsberger, 2006).

I observed that the average diameters in each ganglion were significantly different in cholinergic and noradrenergic neurons in each level of the thoracic ganglia. The noradrenergic cell diameters were significantly different in different levels ($p < 0.0001$). Additionally, there was a significant individual difference in the average sizes of the noradrenergic SPNs in the two subjects ($p < 0.05$). The average cell diameters of noradrenergic and cholinergic SPNs were different according to the segmental level also in the cholinergic population ($p < 0.0001$). There was also a significant individual difference in the average sizes of the cholinergic SPNs in the two subjects ($p < 0.05$). Although we would need a bigger sample size to find a trend along the rostrocaudal axis, our results show segmental differences. The segmental differences in the diameters can be attributed to the number of innervations each level receives from PreSNs (Purves et al., 1986). The SPNs in different levels receive preganglionic innervation from different but overlapping sets of spinal cord segments (Lichtman et al., 1980). The number of

SPNs receiving innervation from a particular level of the spinal cord is different depending on which ganglion they are in.

There is a big individual variation in PSG of many other species, including humans, in terms of size, location, and morphology (Hoffman et al., 1957; Ramsaroop et al., 2001; Kommuru et al., 2014; Dood and Horn, 1983). We can conclude that this is also the case in mice. We found that there was a 3-fold difference in the number of cells in the two animals, and in noradrenergic/cholinergic distributions and cell size distributions. Though we are unsure of the exact reason for the variability between the two samples in this study, two factors could contribute to the difference: 1) sex differences and 2) weight differences.

A study suggested that there is some evidence, though weak, that all sympathetic neurons may be slightly smaller in females than in males **(**Headley et al., 2005). Specifically in the PSG, there are numerous studies that suggest sexual dimorphism in the superior cervical ganglion. Wright (1988) noted that male rats have 20-30% more neurons in the superior cervical ganglia than do females starting from P15. Beaston-Wimmer and Smolen (1991) found that the noradrenergic content per neuron is equal in male and female rats. However, they observed that the males had more TH-mRNA expression. Although Li et al. (2007) did not study the noradrenergic or cholinergic populations specifically, they observed a sex difference in immunoreactivity to neuroendocrine secretory proteins in superior cervical ganglia, stellate ganglia, and thoracic ganglia in rats. If the findings in rats are consistent in mice, the variation in the results of our sample could be attributed to sex.

In analyzing data from six other mice at T3, T5, and T9 ganglia, I showed no change that correlated with sex. This is supported by Pospieszny and Bruzewicz (1998), who noted that there was no perceptible influence of sex on the rate of development of the thoracic sympathetic chain

in pig. Yet, the additional sample also had additional variables, such as spinalization, and several were analyzed using a different counting method.

Alternatively, the difference could be attributed to the weights. As stated above, larger species tend to have more neurons residing in the cervical ganglia (Purves et al., 1985). Our results can be due to the larger body size of male mouse compared to female mouse (Hanrahan and Eisen, 1973). Although, their exact weights were not noted at time of sacrifice, our mice were all less than 22g. Though it cannot be confirmed in our sample, generally male mice are larger than female mice. For example, in a study, 9-14 months old 59 female mice averaged 28.9g and14 males averaged 38.6g, and 17-20months old 51 females averaged 32.9g and 14 males averaged 38.2g (Trentin, 1950). Further experiments in males and females need to be conducted, controlling for the weight, in order to determine the factor that is creating the variation. Understanding the variability of the anatomy of the tPSG may be important for surgical approaches in management of injury or disease.

When applying these findings to future studies, possible errors in this study should be noted. We attempted to avoid sampling error by studying every section. However, the numbers may not reflect the true noradrenergic/cholinergic populations, because there could be error in sectioning of losing certain parts of the tissue. Also, there is unavoidable sectioning artifact that distorts the shape of the cell.

Additionally, when applying these findings to humans, though mice are genetically similar to humans, the differences between the mice and humans reflected upon. One such difference is in the morphology of the SPNs. Mice have less number of primary dendrite, less complexity in dendrites, and less number of innervating axons compared to larger sized mammals (Purves and Lichtman, 1985). Human SPNs have more dendrites, at least 20

preganglionic input converging on each SPN in the SCG (McLachlan, 2003). Another difference is in the sweat glands. Human sweat glands are present in skin all over the body surface, unlike mice that do not have sweat glands on hairy skin. Human sudomotor neurons are involved in thermoregulation (Janig et al, 1982), whereas mouse sudomotor neurons function to increase traction for mobility (Stumpf et al., 2004). Also, human sweat gland innervation is both cholinergic and noradrenergic (Weihe et al., 2005). Attributing the high number of cholinergic SPNs in a certain ganglion to control of sweat in a certain area of the body would be inapparopriate. Lastly, as described in Figure 2, we must be aware that humans and mice have different number of ganglia in different regions of the sympathetic chain.

REFERENCES

Apostolova, G., Dechant, G. (2009) Development of neutrotransmitter phenotypes in sympathetic neurons. *Auton Neurosci*, 151(1): 30-8.

Asamoto, K. (2004) Neural circuit of the cervical sympathetic nervous system with special reference to input and output of the cervical sympathetic ganglia: relationship between spinal cord and cervical sympathetic ganglia and that between cervical sympathetic ganglia and their target organs. *Kaibogak Zasshi*, 79(1): 5-14.

Asmus, S.E., Parsons, S., Landis, S.C. (2000) Developmental changes in the transmitter properties of sympathetic neurons that innervate the periosteum. *J Neurosci*, 20(4): 1495-504.

Beaston-Wimmer, P., Smolen, A.J. (1991) Gender differences in neurotransmitter expression in the rat superior cervical ganglion. *Brain Res Dev Brain Res*, 58(1): 123-8.

Blackman, J.G., Purves, R.D. (1969) Intracellular recordings from ganglia of the thoracic sympathetic chain of the guinea-pig. J Physiol, 203(1): 173-98.

Boyd, H.D., McLachlan, E.M., Keast, J.R., Inokuchi, H. (1996) Three electrophysiological classes of guinea pig sympathetic postganglionic neurone have distinct morphologies. *J Comp Neurol*, 369(3): 372-387.

Bowers, C.W., Zigmond, R.E. (1979) Localization of neurons in the rat superior cervical ganglion that project into different postganglionic trunks. *J Comp Neurol*, 185(2): 381-91.

Buckley, G., Consolo, S., Giacobini, E., Sjoqvist, F. (1967) Cholinacetylase in innervated and denervated sympathetic ganglia and ganglion cells of the cat. *Acta physiol. scand.*, 71: 348-356.

Burnstock, G. (1969) Evolution of the autonomic innervation of visceral and cardiovascular systems in vertebrates. Pharmacol Rev, 21(4): 247-324.

Dale, H. (1937) Transmission of nervous effects by acetylcholine. *Bull N Y Acad Med*, 13(7): 379-396.

Dodd, J., Horn, J.P. (1983) A reclassification of B and C neurones in the ninth and tenth paravertebral sympathetic ganglia of the bullfrog. *J Physiol*, 334: 255-269.

Dehal, N.S., Kartseva, A., Weaver, L.C. (1992) Comparison of locations and peptide content of postganglionic neurons innervating veins and arteries of the rat hindlimb. *J Auton Nerv Syst*, 39(1): 61-72.

Elfvin, L.G., Lindh, B., Hokfelt, T. (1993) The chemical neuroanatomy of sympathetic ganglia. *Annu Rev Neurosci*, 16: 471-507.

Ernsberger, U., Rohrer, H. (1999) Development of the cholinergic neurotransmitter phenotype in postganglionic sympathetic neurons. *Cell Tissue Res*, 297: 339-361.

Ernsberger, U., Reissmann, E., Mason, I., Rohrer, H. (2000) The expression of dopamine β-hydroxylase, tyrosine hydroxylase, and Phox2 transcription factors in sympathetic neurons: evidence for common regulation during noradrenergic induction and diverging regulation later in development. *Mech Dev*, 92(2): 169-177.

Falck, B., Hillarpy, N.A., Tieme, G., Torp, A. (1962) *Histochemistry and Cell Biology of Autonomic Neurons, SIF Cells and Paraneurons.* New York: Raven.

Flett, D.L., Bell, C. (1991) Topography of functional subpopulations of neurons in the superior cervical ganglion of the rat. *J Anat*, 177: 55-66.

Forehand, C.J., Ezerman, E.B., Rubin, E., Glover, J.C. (1994) Segmental patterning of rat and chicken sympathetic preganglionic neurons: correlation between soma position and axon projection pathway. *J Neurosci*, 14(1): 231-241.

Francis, N.J., Landis, S.C. (1999) Cellular and molecular determinants of sympathetic neuron development. *Annu Rev Neurosci*, 22: 541-66.

Garry, T.P., Henry A.K. (1949) Anterior transcoastal access to upper parts of the thoracic sympathetic chain. *Ir J Med Sci*, 286: 757-61.

Gibbins, I.L. (1991) Vasomotor, pilomotor and secretomotor neurons distinguished by size and neuropeptide content in superior cervical ganglia of mice. *J Auton Nerv Syst*, 34(2-3): 171-183.

Gibbins, I.L. (1992) Vasoconstrictor, vasodilator and pilomotor pathways in sympathetic ganglia of guinea-pigs. *Neuroscience*, 47(3): 657-672.

Gibbins, I.L., Rodgers, H.F., Matthew, S.E., Murphy, S.M. (1998) Synaptic organisation of lumbar sympathetic ganglia of guinea pigs: serial section ultrastructural analysis of dye-filled sympathetic final motor neurons. *J Comp Neurol*, 402(3): 284-302.

Gibbins, I.L., Jobling, P., Messenger, J.P., Teo, E.H., Morris, J.L. (2000) Neuronal morphology and the synaptic organisation of sympathetic ganglia. *J Auton Nerv Syst*, 81(1-3): 104-9.

Glebova, N.O. and Ginty, D.D. (2005) Growth and survival signals controlling sympathetic nervous system development. *Annual Review of Neuroscience*, 28: 191-222.

Goodall, M., Kirshner, N. (1958) Biosynthesis of epinephrine and norepinephrine by sympathetic nerves and ganglia. *Circulation,* 17(3): 366-71.

Habecker, B.A., Landis, S.C. (1994) Noradrenergic regulation of cholinergic differentiation. *Science*, 264(5165): 1602-4.

Hanrahan, J.P., Eisen, E.J. (1973) Sexual dimorphism and direct and maternal genetic effects on body weight in mice. *Theor Appl Genet,* 43(1): 39-45.

Headley, D.B., Suhan, N.M, Horn, J.P. (2005) Rostro-caudal variations in neuronal size reflect the topography of cellular phenotypes in the rat superior cervical sympathetic ganglion. Brain Res, 1057(1-2): 98-104.

Hill, C.E., Burnstock, G. (1975) Amphibian sympathetic ganglia in tissue culture. *Cell Tiss Res*. 162: 209-233.

Hill, E.L., Elde, R. (1989) Vasoactive intestinal peptide distribution and colocalization with dopamine-beta-hydroxylase in sympathetic chain ganglia of pig. *J Auton Nerv Syst*. 27(3): 229-239.

Hoffman, H.H. (1957) An analysis of the sympathetic trunk and rami in the cervical and upper thoracic regions in man. *Ann Surg*, 145(1): 94-103.

Holmstedt, B. and Sjoqvist, F. (1959) Distribution of acetocholinesterase in the ganglion cells of various sympathetic ganglia. *Acta Phsyiol Scand*, 47: 284-296.

Honma, S. (1970) Histochemical demonstration of catecholamines in the toad sympathetic ganglia. *Jpn J Physiol*, 20(2): 186-97.

Hou, S., Duale, H., Rabchevsky, A.G. (2009) Intraspinal sprouting of unmyelinated pelvic afferents after complete spinal cord injury is correlated with autonomic dysreflexia induced by visceral pain. *Neuroscience,*159:369-379.

Huber, K., Ernsberger, U. (2006) Cholinergic differentiation occurs early in mouse sympathetic neurons and requires Phox2b. Gene Expr. 13(2): 133-9.

Janig, W., Krauspe, R., Wiedersatz, G. (1982) Transmission of impulses from pre- to postganglionic vasoconstrictor and sudomotor neurons. *J Auton Nerv Syst*, 6(1): 95-106.

Janig, W., Habler, H.J. (2003) Neurophysiological analysis of target-related sympathetic pathways--from animal to human: similarities and differences. *Acta Physiol Scand*, 177(3): 255-74.

Jacobowitz, D., Woodward, J.K. (1968) Adrenergic neurons in the cat superior cervical ganglion and cervical sympathetic nerve trunk. A histochemical study. *J Pharmacol Exp Ther*, 162(2): 213-26.

Jobling, P., Gibbins, I.L. (1999) Electrophysiological and morphological diversity of mouse sympathetic neurons. *J Neurophysiol*, 82(5): 2747-64.

Karlsson, A.K. (1999) Autonomic dysreflexia. *Spinal Cord*, 44: 341-351.

Keast, J.R., Luckensmeyer, G.B., Schemann, M. (1995) All pelvic neurons in male rats contain immunoractivity for the synthetic enzymes of either noradrenaline or acetylcholine. *Neuroscience Letters*, 196(2): 209-212.

Kesse, W.K., Parker, T.L., Coupland, R.E. (1988) The innervation of the adrenal gland I. The source of pre- and postganglionic nerve fibres to the rat adrenal gland. *J Anat*, 157: 33-41.

Klimaschewski, L., Kummer, W., Heym, C. (1996) Localization, regulation, and functions of neurotransmitters and neuromodulators in cervical sympathetic ganglia. Microscopy Research and Technique, 35: 44-68.

Koelle, G.B., Friedenwald, J.S. (1949) A histochemical method for localizing cholinesterase activity. *Exp Biol Med (Maywood)*, 70(4): 617-622.

Kommuru, H., Jothi, S., Bapuji, P., Sree, D.L., Antony, J. (2014) Thoracic part of sympathetic chain and its branching pattern variations in South Indian cadavers. *J Clin Diagn Res*, 8(12): AC09-12.

Langley, J.N. (1921) *The Autonomic Nervous System*, Cambridge: Heffer.

Landis, S.C. and Fredieu, J.R. (1986) Coexistence of calcitonin gene-related peptide and vasoactive intestinal peptide in cholinergic sympathetic innervation of rat sweat glands. *Brain Res*, 377(1): 177-81.

Landis, S.C. and Keefe, D. (1983) Evidence for neurotransmitter plasticity in vivo: developmental changes in properties of cholinergic sympathetic neurons. *Dev Biol*, 98(2): 349-72.

Lascar, G., Eugene, D., Taxi, J. (1996) Synaptic organization of amphibian sympathetic ganglia. *Microsc Res Tech*, 35(2): 157-78.

Li, Y., Wang, Z., Dahlstrom, A. (2007) Neuroendocrine secretory protein 55 (NESP55) immunoreactivity in male and female rat superior cervical ganglion and other sympathetic ganglia. *Auton Neurosci*, 132(1-2): 52-62.

Lichtman, J.W., Purves, D., Yip, J.W. (1979) On the purpose of selective innervation of guinea-pig superior cervical ganglion cells. *J Physiol*, 292: 69-84.

Lichtman, J.W., Purves D., and Yip J.W. (1980) Innervation of sympathetic neurons in the guinea-pig thoracic chain. *J Physiol*, 298: 285-299.

Lindh, B., Hokfelt, T., Elfvin, L.G., Terenius, L., Fahrenkrug, J., Elde, R., Goldstein, M. (1986a) Topography of NPY-, somatostatin-, and VIP-immunoreactive, neuronal subpopulations in the guinea pig celiac-superior mesenteric ganglion and their projection to the pylorus. *J Neurosci*, 6(8): 2371-2383.

Lindh, B., Staines, W., Hokfelt, T., Terenius, L., Salavaterra, P.M. (1986b) Immunohistochemical demonstration of choline acetyltransferase-immunoreactive preganglionic nerve fibers in guinea pig autonomic ganglia. *Proc Natl Acad Sci U S A,* 83(14): 5316-20.

Loesel, R., Weigel, S., Braunig, P. (2006) A simple fluorescent double staining method for distinguishing neuronal from non-neuronal cells in the insect central nervous system. *J Neurosci Methods*, 155(2): 202-6.

Marshall, W.F., Young, K.D., Swaffer, M., Wood, E., Nurse, P., Kimura, A., Frankel, J., Wallingford, J., Walbot, V., Qu, X., Roeder, A.H. (2012) What determines cell size? *BMC Biol*, doi: 10.1186/1741-7007-10-101.

Masliukov, P.M. and Timmermans, J.P. (2004) Immunocytochemical properties of stellate ganglion neurons during early postnatal development. *Histochem Cell Biol*, 122:201-209.

Matthews, M.R., Raisman, G. (1972) A light and electron microscopic study of the cellular response to axonal injury in the superior cervical ganglion of the rat. *Proc R Soc Lond B Biol Sci*, 181(1062) 43-79.

McLachlan, E.M. (2003) Transmission of signals through sympathetic ganglia--modulation, integration or simply distribution? *Acta Physiol Scand*, 177(3): 227-35.

Morales, M.A., Holmberg, K., Xu, Z.Q., Cozzari, C., Hartman, B.K., Emson, P., Goldstein, M., Elfvin, L.G., Hokfelt, T. (1995) Localization of choline acetyltransferase in rat peripheral sympathetic neurons and its coexistence with nitric oxide synthase and neuropeptides. Proc Natl Acad Sci U S A, 92(25): 11819-23.

Muller, B., Harris, T., Borri Voltattorni, C., and Bell, C. (1984) Distribution of neurones containing dopa decarboxylase and dopamine-beta-hydroxylase in some sympathetic ganglia of the dog: a quantitative study. *Neuroscience*, 11: 733-740.

Mustonen, T., Pispa, J., Mikkola, M.L., Pummila, M., Kangas, A.T., Pakkasjarvi, L., Jaatinen, R., Thesleff, I. (2003) Stimulation of ectodermal organ development by Ectodysplasin-A1. *Dev Biol*, 259(1): 123-36.

Naftel, J.P., Hardy S.G.P. (2006) Visceral motor pathways. In *Fundamental Neuroscience for Basic and Clinical Applications*, 3: 405-416.

Nagatsu, T., Levitt, M., Udenfriend, S. (1964) Tyrosine hydroxylase. The initial step in norepinephrine biosynthesis. *J Biol Chem*, 239: 2910-7.

Nja, A., Purves, D. (1977) Specific innervation of guinea-pig superior cervical ganglion cells by preganglionic fibres arising from different levels of the spinal cord. J Physiol, 264(2): 565-583.

Nozdrachev, A.D., Jimenez, B., Morales, M.A. (2002) Neuronal organization and cell interactions of the cat stellate ganglion. *Autonomic Neuroscience*, 95(1-2): 43-56.

Parker, T.L., Mohamed, A.A., Coupland, R.E. (1990) The innervation of the adrenal gland. IV. The source of pre- and postganglionic nerve fibres to the guinea-pig adrenal gland. *J Anat*, 172: 17-24.

Pattyn, A., Morin, X., Cremer, H., Goridis, C., Brunet, J.F. (1999) The homeobox gene Phox2b is essential for the development of autonomic neural crest derivatives. Nature, 399(6734): 366-79.

Phifer-Rixey, M. and Nachman, M. (2015) Insights into mammalian biology from the wild house mouse Mus Musculus. *eLife*, 4(e05959).

Pospieszny, N., Bruzewicz, S. (1998) Morphology and development of the thoracic part of the sympathetic trunk (pars thoracica trunci sympathici) in the pig (Sus scrofa L.) during the prenatal period. *Ann Anat*, 180(1): 87-91.

Purves, D., Hume R.I. (1981) The relation of postsynaptic geometry to the number of presynaptic axons that innervate autonomic ganglion cells. *J Neurosci*, 1:441-452.

Purves, D., Lichtman, J.W. (1985) Geometrical differences among homologous neurons in mammals. *Science*, 228(4697): 298-302.

Purves, D., Rubin, E., Snider, W.D. and Lichtman, J. (1986) Relation of animal size to convergence, divergence, and neuronal number in peripheral sympathetic pathways. *J Neurosci*, 6(1): 158-163.

Rabchevsky, A.G. (2006) Segmental organization of spinal reflexes mediating autonomic dysreflexia after spinal cord injury. *Prog Brain Res*, 152: 265-274.

Ramsaroop, L., Partab, P., Singh, B., Satyapal, K.S. (2001) Thoracic origin of a sympathetic supply to the upper limb: the 'nerve of Kuntz' revisited. *J Anat*, 199(6): 675-82.

Rao, M.S., Jaszczak, E., Landis, S.C. (1994) Innervation of footpads of normal and mutant mice lacking sweat glands. *J Comp Neurol*, 346(4): 613-25.

Schafer, M.K., Schutz B., Weihe, E., Eiden, L.E. (1997) Target-independent cholinergic differentiation in the rat sympathetic nervous system. *Proc Natl Acad Sci U S A*, 94(8): 4149-54.

Schafer, M.K., Eiden, L.E., Weihe, E. (1998) Cholinergic neurons and terminal fields revealed by immunohistochemistry for the vesicular acetylcholine transporter. II. The peripheral nervous system. *Neuroscience*, 84(2): 351-376.

Schotzinger, R.J., Landis, S.C. (1988) Cholinergic phenotype developed by noradrenergic sympathetic neurons after innervation of a novel cholinergic target in vivo. *Nature,* 335(6191): 637-9.

Schotzinger, R.J., Landis, S.C. (1990) Acquisition of cholinergic and peptidergic properties by sympathetic innervation of rat sweat glands requires interaction with normal target. *Neuron,* 5(1): 91-100.

Schotzinger, R., Yin, X., Landis, S. (1994) Target determination of neurotransmitter phenotype in sympathetic neurons. *J Neurobiol*, 25(6): 620-39.

Schutz, B., von Engelhardt, J., Gordes, M., Schafer, M.K., Eiden, L.E., Monyer, H., Weihe, E. (2008) Sweat gland innervation is pioneered by sympathetic neurons expressing a cholinergic/noradrenergic co-phenotype in the mouse. *Neuroscience,* 156(2): 310-8.

Scrivener, Y., Cribier, B. (2002) Morphology of sweat glands. *Morphologie*, 86(272): 5-17.

Sjoqvist, F. (1962) Morphological correlate to a cholinergic sympathetic function. *Nature*, 195(298).

Sjoqvist, F. (1963) Pharmacological analysis of acetylcholinesterase-rich ganglion cells in the lumbo-sacral sympathetic system of the cat. *Acta physiol. scand.*, 57: 339-351.

Semenenko, F.M., Cuello, A.C., Goldstein, M., Lee, K.Y., Sidebottom, E. (1986) A monoclonal antibody against tyrosine hydroxylase: application in light and electron microscopy. *J Histochem Cytochem*, 34(6): 817-21.

Smolen, A.J., (1988) Morphology of synapses in the autonomic nervous system. *J Electron Microsc Tech*, 10(2): 187-204.

Srivastava, V., Ow, D. (2015) Simplifying transgene locus structure through Cre-lox recombination. *Methods Mol Biol*, 1287: 95-103.

Stumpf, P., Kunzle, H., Welsch, U. (2004) Cutaneous eccrine glands of the foot pads of the small Madagascan tenrec (Echinops telfairi, Insectivora, Tenrecidae): skin glands in a primitive mammal. *Cell Tissue Res*, 315(1): 59-70.

Taylor, D.K., Bubler, J.A., Silva, K.A. and Sundberg J.P. (2012) Development, structure, and keratin expression in C57BL/6J mouse eccrine glands. *Vet Pathol*, 49(1): 146-54.

Teitelman, G., Baker, H., Joh, T.H., Reis, D.J. (1979) Appearance of catecholamine-synthesizing enzymes during development of rat sympathetic nervous system: Possible role of tissue environment. *Proc Natl Acad Sci U S A*, 76(1): 509-513.

Trentin, J.J. (1950) Sex difference in the effect of progesterone on body weight of mice. *Proc Soc Exp Biol Med,* 75(1): 267-9.

Voyvodic, J.T. (1987) Development and regulation of dendrites in the rat superior cervical ganglion. *J Neurosci*, 7(3): 904-912.

Weihe, E., Eiden, L.E. (2000) Chemical neuroanatomy of the vesicular amine transporters. *FASEB J*, 14(15): 2435-49.

Weihe, E., Schutz, B., Hartschuh, W., Anlaug, M., Schafer, M.K. and Eiden, L.E. (2005) Co-expression of cholinergic and noradrenergic phenotypes in human and non-human autonomic nervous system. *J Comp Neurol*, 492(3): 370-379.

Wright, L.L. (1988) Gender difference in a subpopulation of rat superior cervical ganglion neurons. *J Auton Nerv Syst*, 22(1): 31-40.

Yip, J.W. (1986) Specific innervation of neurons in the paravertebral sympathetic ganglia of chick. *J Neurosci*, 6(12): 3459-3464.